De Troianis: The Trojans in the Planetary System

Elisabetta Dotto
INAF, Osservatorio Astronomico di Roma

Joshua P. Emery
NASA Ames Research Center/SETI Institute

Maria A. Barucci
LESIA, Observatoire de Paris

Alessandro Morbidelli
Observatory of Nice

Dale P. Cruikshank
NASA Ames Research Center

Trojan objects are minor bodies having stable orbits in the L_4 and L_5 Lagrangian points of a planet. Mars, Jupiter, and Neptune are known to support Trojans, but Saturn and Uranus are also believed to share their orbits with similar populations of small bodies. Recent dynamical modeling suggests a genetic relationship among transneptunian objects (TNOs) and Jupiter and Neptune Trojans: All these bodies are believed to have formed at large heliocentric distances in a region rich in frozen volatiles. In this context, the analysis and the comparison of the physical properties of Trojans, Centaurs, and TNOs can help us to constrain the link among them and the scenario of the planetary formation in the outer solar system. This chapter presents an overview of current knowledge of the physical properties of Trojans. Since the Jupiter Trojans are the most well studied of the Trojan populations, discussion is centered on the analysis of the properties of this group and comparison with asteroids, comets, Centaurs, and TNOs. The physical characteristics of Jupiter Trojans share some similarities with those of the other populations of small bodies of the outer solar system, but also some notable differences. Some analogies with neutral/less-red Centaurs suggest that Jupiter Trojans are more similar to the active and post-active comets than to the non-active icy bodies. This may support a genetical link among these objects, but the complete puzzle is still far from being understood.

1. INTRODUCTION

Why a chapter devoted to the Trojans in a book on transneptunian objects (TNOs)? The answer to this question comes from the observational evidence of some similarities in the physical characteristics of Jupiter Trojans, TNOs, short-period comets, and Centaurs, and from recent dynamical modeling that suggests that Jupiter Trojans originated in the primordial transneptunian disk.

The objects located in the L_4 and L_5 Lagrangian points of a planet's orbit are called Trojans. To date, Lagrangian bodies have been discovered in the orbits of Mars, Jupiter, and Neptune. The identification of Mars Trojans is still a matter of debate: Only four objects have been confirmed to be in the Mars Lagrangian points (*Scholl et al.,* 2005), and several other bodies have been identified as potential Mars Trojans. Although the population of Neptune Trojans is expected to be 20 times larger than that of Jupiter Trojans (*Sheppard and Trujillo,* 2006a), only six objects are known so far. At present, the most numerous group of known Trojans is in the orbit of Jupiter. It includes more than 2250 objects, about 1230 in the L_4 cloud and about 1050 in the L_5 cloud.

The absolute magnitude distribution of Jupiter Trojans has been the object of a study by *Jewitt et al.* (2000), with observations targeted at the discovery of faint objects. They found that the absolute magnitude (H) distribution of objects with $11 < H < 16$ is exponential, with an exponent $\alpha = 0.4 \pm 0.3$. Assuming that albedo is independent of size, this implies that the cumulative size distribution is a power law with an exponent $q = -2.0$. On the bright end of the distribution, the observations cataloged at the time allowed the authors to infer that the absolute magnitude distribution is much steeper, with an exponent $\alpha = 5.5 \pm 0.9$. In order to estimate a total population, the measurements have to be corrected for the incompleteness of the survey, which is a difficult process. Jewitt et al. only surveyed a small fraction of the L_4 swarm. They estimated the surface density distribution of Trojans (as a function of the angle from the L_4 point) as a Gaussian fit to their data, and used this fit to

correct for the incompleteness of their survey. They then multiplied by a factor of 2 to account for the L_5 swarm as well. Jewitt et al. concluded that the rollover from the steep distribution at the bright end to the shallow distribution at the faint end occurs around H ~ 10, and that the total number of Trojans brighter than H = 16 is ~10^5. The situation has evolved since 2000, thanks to the enhanced discovery rate due to the new asteroid surveys such as LINEAR. An updated catalog (see, e.g., *hamilton.dm.unipi.it/cgi-bin/astdys/astibo*) shows more objects than considered by Jewitt et al. for H < 9 and fewer objects at fainter magnitudes. *Yoshida and Nakamura* (2005) performed a survey of L_4 for faint Trojans similar to that of *Jewitt et al.* (2000). They find a cumulative H-distribution slope of 1.89 ± 0.1, which agrees very well with the value found by Jewitt et al. Furthermore, they note an apparent change in slope at H ~ 16 (D ~ 5 km for p_v = 0.04), which is similar to a change in slope discovered for small main-belt asteroids (*Ivezić et al.,* 2001; *Yoshida et al.,* 2003). The *Yoshida and Nakamura* (2005) search area was small, and they used the same surface density correction for the incompleteness of their survey as that used by *Jewitt et al.* (2000). Their final distribution results in about three times more Trojans larger than 1 km than the Jewitt et al. estimate, although it is not clear what distribution they used for the bright (H < 14) objects. According to recent results from the Sloan Digital Sky Survey (SDSS) (*Szabó et al.,* 2007), the L_4 swarm seems to contain significantly more asteroids than the L_5 one. The Trojan catalog is complete up to absolute magnitude H = 13.8 (corresponding to a diameter of about 10 km). Beyond this threshold, SDSS detections confirm the slope of the H distribution found by *Jewitt et al.* (2000). This implies that the number of Jupiter Trojans is about the same as that of the main-belt asteroids down to the same size limit.

About 3% of Jupiter Trojans are on unstable orbits having eccentricities larger than 0.10 and inclinations greater than 55°. Nevertheless, the orbits of the majority of Jupiter Trojans are stable over the age of the solar system (*Levison et al.,* 1997; *Giorgilli and Skokos,* 1997). The population as a whole is widely believed to be as collisionally evolved as the asteroid main belt, and the recent discovery of dynamical families (*Shoemaker et al.,* 1989; *Milani,* 1993; *Milani and Knežević,* 1994; *Beaugé and Roig,* 2001) confirms this hypothesis.

While the dynamical characteristics are quite well determined, the physical properties of the Mars, Jupiter, and Neptune Trojan populations are not as well known. *Rivkin et al.* (2003) carried out visible and near-infrared spectroscopy of three out of the four confirmed Mars Trojans, finding large spectral differences: 5261 Eureka and 101429 1998 VF_{31} have been classified as Sr (or A) type and Sr (or Sa) type, respectively, while 121514 1999 UJ_7 belongs to the X (or T) class. These results seem to suggest that these objects did not all form in their current locations, or alternatively they suffered a strong variation in their sizes.

Color measurements of Neptune Trojans have shown that they are statistically indistinguishable from one another with slightly red colors, similar to the Jupiter Trojans and neutral/less-red Centaurs. On the basis of this result, *Sheppard and Trujillo* (2006b) argued that Neptune Trojans had a common origin with Jupiter Trojans, irregular satellites, and the dynamically excited gray Kuiper belt population, and are distinct from the classical Kuiper belt objects. For Jupiter Trojans, we have visible color indexes of about 300 objects, visible spectra of less than 150 bodies, near-infrared spectra of a sample of about 50 objects (see section 3.4), and thermal-IR spectra of only 3 bodies (see section 3.5). Albedo values are known for a few tens of objects, mainly published by *Fernández et al.* (2003), while only two measurements of the density are available in the literature so far (*Lacerda and Jewitt,* 2006; *Marchis et al.,* 2006a,b). On the basis of this still incomplete sample of information, the population of Jupiter Trojans shows some similarities, together with some differences, with the other populations of minor bodies of the outer solar system. Comparison among the physical and dynamical properties of the Jupiter Trojans, and those of Centaurs, TNOs, and outer dwarf planets, although challenging, is necessary to constrain the scenario of the formation and early evolution of the outer part of the solar system, and give an answer to the still open questions of where these bodies formed and how they evolved.

2. ORIGIN AND POSSIBLE DYNAMICAL LINK BETWEEN JUPITER TROJANS AND TRANSNEPTUNIAN OBJECTS

There are two models for the origin of Jupiter Trojans. Each model has distinct implications for the composition of these objects, and therefore distinct implications for similarities and differences between Trojans and TNOs.

The first model, which we will call "classical" as it remained unchallenged until 2005, considers that the Trojans originally were planetesimals formed in the vicinity of Jupiter's orbit. They were captured on tadpole orbits (namely on orbits that librate around the Lagrange equilateral equilibrium points L_4 and L_5) when Jupiter's gravity abruptly increased due to the accretion of a massive atmosphere (pull-down mechanism) (*Marzari and Scholl,* 1998a,b; *Fleming and Hamilton,* 2000). Assuming a time evolution of Jupiter's mass as in *Pollack et al.* (1996), *Marzari and Scholl* (1998a,b) showed with numerical simulations that this capture mechanism is very efficient: Between 40% and 50% of the planetesimals populating a ring extending 0.4 AU around Jupiter's orbit can be captured as Trojans. After capture, the angular amplitude of libration shrinks by a factor $(M_J = M_{J,c})^{-1/4}$, as Jupiter's mass continues to grow, M_J and $M_{J,c}$ denoting the mass of Jupiter at the current time and at the time of capture, respectively (*Fleming and Hamilton,* 2000). Gas drag could also help in the capture of Trojans from the local planetesimal population, but is effective only for the small objects (*Peale,* 1993).

The problem with the classical model is that the resulting orbital distribution of the Trojans is not, at first sight, very similar to the observed one. The captured Trojans typically

have large libration amplitudes, despite the partial damping process mentioned above. Conversely, the observed objects have a fairly uniform libration amplitude distribution. Using a Monte Carlo method, *Marzari and Scholl* (1998b) showed that collisions can significantly alter the distribution of libration amplitudes by injecting initially large librators into more-stable, small-libration-amplitude orbits. In addition, the Trojans with the largest libration amplitudes would tend to escape by chaotic diffusion over the age of the solar system (*Levison et al.,* 1997). Thus, the libration amplitude distribution resulting from the pull-down mechanism might be reconciled with the observed distribution, invoking the subsequent collisional and dynamical evolution.

A more serious disagreement concerns the inclination distributions. The pull-down mechanism does not significantly affect the eccentricities and the inclinations of the planetesimals. Thus the eccentricity and inclination distributions of the captured Trojans should be reminiscent of those of the planetesimal disk. Because the disk was dynamically stirred by the presence of Jupiter's core, the eccentricities and inclinations of the local planetesimals are not expected to be very small. However, they are not expected to be large either, because the bodies kicked to large eccentricity/inclination orbits by encounters with the proto-Jupiter were most likely displaced (in semimajor axis) from Jupiter's orbit, so that they could not be captured by the pull-down mechanism. The observed eccentricity distribution of Trojans ranges from 0 to ~0.15 [the latter being a sort of dynamical stability limit (*Rabe,* 1965; *Levison et al.,* 1997; *Robutel and Gabern,* 2006)], so it might not be a problem. However, the observed inclination distribution ranges up to about 40°, well beyond expectations from the local capture model. *Marzari and Scholl* (2000) showed that the inclination can be excited up to 20°–30° by the secular resonance ν_{16}, which occurs when the longitude of the node of a Trojan precesses at the same rate of those of Jupiter and Saturn (which are equal to each other). The problem is that this resonance operates only on Trojans with a libration amplitude of about 30° (here the libration amplitude is defined as the half-difference between the minimal and the maximal value of $\lambda_T - \lambda_J$, where λ denotes the mean longitude of a body and the subscript T and J refer to the Trojan and Jupiter, respectively). Another possibility, in analogy with the asteroid belt excitation/depletion model of *Wetherill* (1992) and *Petit et al.* (2001), is that the primordial Trojan population contained massive planetary embryos, which excited the inclinations of the smaller objects by repeated encounters, up to the time when they eventually escaped from the Trojan region due to their mutual interactions. The problem with this model is that, because the inclination distribution of the Trojans around the L_4 and L_5 points are similar, almost equal populations of embryos should have orbited in the two Trojan regions, and for about the same time, which seems unlikely from a probabilistic point of view.

A full simulation of the Trojan capture process by the pull-down mechanism, including the effects of collisional damping, secular resonance excitation, and/or the presence of massive planetary embryos, has never been done. Thus, it has never been shown that the local capture model can satisfactorily reproduce the orbital distribution of the observed Trojans.

An alternative model for the origin of the Trojans has been recently proposed (*Morbidelli et al.,* 2005). It also invokes the capture of Trojans, but from a more distant disk. The latter should be identified with the primordial transneptunian disk, which is also the ancestor of the Kuiper belt. The model assumes that initially Saturn was closer to Jupiter than their mutual 1:2 mean-motion resonance, and invokes the well-known migration of the giant planets due to their interaction with the disk of planetesimals (*Fernández and Ip,* 1984; *Malhotra,* 1993, 1995; *Hahn and Malhotra,* 1999, 2005; *Gomes et al.,* 2004). During their migration in divergent directions, Jupiter and Saturn eventually had to cross the 1:2 resonance. It is known from *Gomes* (1997) and *Michtchenko et al.* (2001) that, if and when this happened, the jovian Trojan region had to become fully unstable. Consequently, any preexisting jovian Trojans would have left the coorbital region.

However, the dynamical evolution of a gravitating system of objects is time-reversible. Thus, if the original objects can escape the Trojan region when the latter becomes unstable, other bodies can enter the same region and be temporarily trapped. Consequently, a transient Trojan population can be created if there is an external source of objects. In the *Morbidelli et al.* (2005) scenario, the source consists of the very bodies that are forcing the planets to migrate, which must be a very large population given how much the planets had to move. When Jupiter and Saturn get far enough from the 1:2 resonance, so that the coorbital region becomes stable again, the population that happens to be there at that time remains trapped. It becomes the population of permanent jovian Trojans still observable today.

This possibility has been tested with numerical simulations in *Morbidelli et al.* (2005). Among the particles that were Jupiter or Saturn crossers during the critical period of Trojan instability, between 2.4×10^{-6} and 1.8×10^{-5} remained permanently trapped as jovian Trojans. Given the mass of the planetesimals that is required in order to move Jupiter and Saturn over the semimajor axis range corresponding to Trojan's instability, this corresponds to a captured Trojan population of total mass between $\sim 4 \times 10^{-6}$ and $\sim 3 \times 10^{-5}\ M_\oplus$. Previous estimates (*Jewitt et al.,* 2000) from detection statistics concluded that the current mass of the Trojan population is $\sim 10^{-4}\ M_\oplus$. However, taking into account modern, more-refined knowledge of the Trojans' absolute magnitude distribution (discussed in *Morbidelli et al.,* 2005), mean albedo (*Fernández et al.,* 2003), and density (see section 3.3), the estimate of the current mass of Trojan population is reduced to $7 \times 10^{-6}\ M_\oplus$, consistent with the mass achieved in the capture simulations.

More importantly, at the end of the simulations, the distribution of the trapped Trojans in the space of the three fundamental quantities for Trojan dynamics — the *proper* eccentricity, inclination, and libration amplitude (*Milani,*

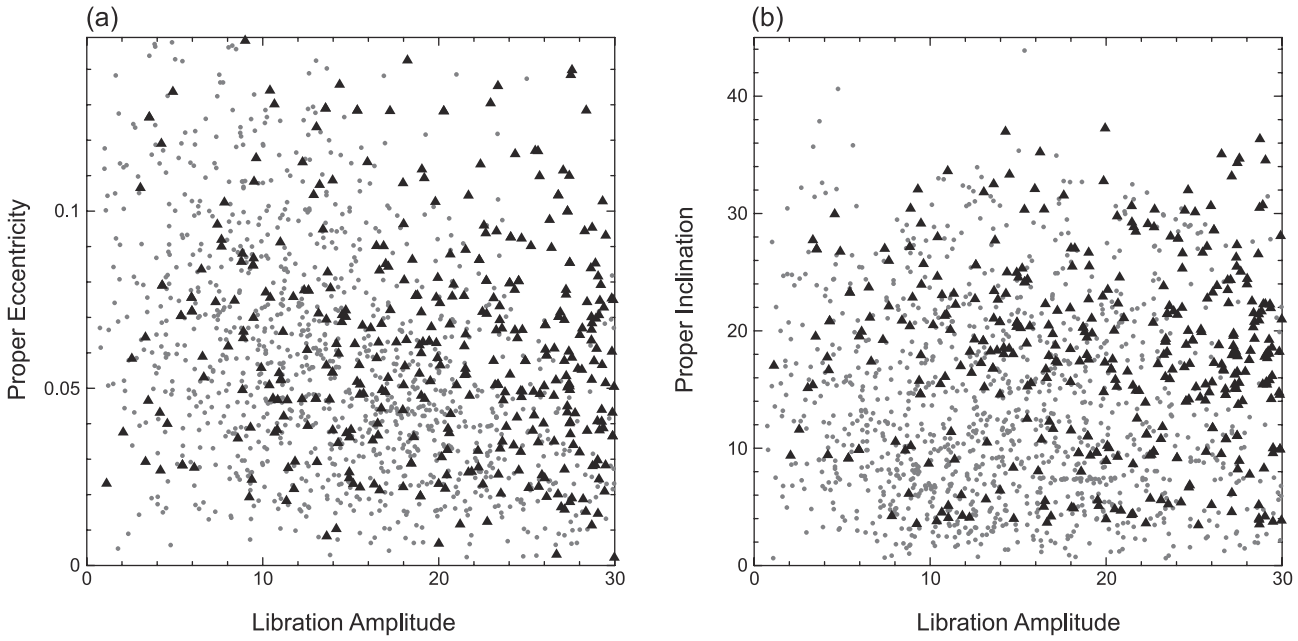

Fig. 1. Comparison of the orbital distribution of Trojans between the simulations in *Morbidelli et al.* (2005) and observations. The simulation results are shown as black triangles and the observations as gray dots in the planes of **(a)** proper eccentricity vs. libration amplitude and **(b)** proper inclination vs. libration amplitude. The distribution of the simulated Trojans is somewhat skewed toward large libration amplitudes, relative to the observed population. However, this is not a serious problem because a fraction of the planetesimals with the largest amplitudes would leave the Trojan region during the subsequent 4 G.y. of evolution (*Levison et al.,* 1997), leading to a better match. The similarity between the two inclination distributions provides strong support for this model of the origin of Trojans.

1993) — was remarkably similar to the current distribution of the observed Trojans, as illustrated in Fig. 1. In particular, this is the only model proposed thus far that explains the inclination distribution of jovian Trojans. This model also predicts that, before being captured in the Trojan region, the objects typically evolved through a large eccentricity phase that brought them relatively close to the Sun. In fact, in the simulations all particles reached temporarily perihelion distance q less than ~3 AU before capture. Of them, 72% spent more than 10,000 yr on orbits with $q < 3$ AU, and 68% even reached $q < 2$ AU. Since it may take roughly 10,000 yr for an active Jupiter-family comet to become dormant (*Levison and Duncan,* 1997), it is possible that the surfaces of the Trojans could have been devolatilized during their high-eccentricity phase. We will return to this issue in section 4.

The positive results of the *Morbidelli et al.* (2005) simulations provide by themselves a strong argument in favor of the passage of Jupiter and Saturn through their mutual 1:2 mean-motion resonance. Additional support comes from the fact that this transition through the resonance explains the orbital excitation of the giant planets' orbits, starting from perfectly circular ones (*Tsiganis et al.,* 2005). Moreover, *Gomes et al.* (2005) showed that, with reasonable assumptions, the passage through the resonance could have occurred after hundreds of millions of years of slow planetary migration, which provides a mechanism for the origin of the otherwise mysterious late heavy bombardment of the terrestrial planets (see *Hartmann et al.,* 2000, for a review). Finally, the orbital architecture of the Kuiper belt also seems to be consistent with the orbital evolution of the planets subsequent to the 1:2 mean-motion resonance crossing (see chapter by Morbidelli et al.). Therefore, the strength of *Morbidelli et al.* (2005) scenario is that it is cast in a more general framework, which is consistent with a large body of constraints given by the solar system's structure.

3. THE PHYSICAL PROPERTIES OF JUPITER TROJANS

As mentioned above, the analysis of the physical similarities and differences between Jupiter Trojans, Centaurs, and TNOs is of fundamental importance to investigations of the possible link among these populations of the outer solar system.

3.1. Rotational Properties

Planetary rotation is the result of the angular momentum added by mutual collisions to the initial angular momentum determined by formation processes. For this reason measurements of rotational properties can provide important clues about the history and evolution of the small-body population. Even though radar and adaptative optics have recently emerged as powerful sources of information, light-curve observations still represent the basic tool for deter-

mining the rotational properties of small bodies, allowing determination of the rotation rate, axis direction, and an approximation of the body shape.

Starting in 1969, Dunlap and Gehrels observed 624 Hektor and revealed a body with a very elongated shape. *Hartmann et al.* (1988) published lightcurves of 18 Trojans, which, on average, had higher amplitudes than main-belt asteroids. They suggested that elongated shapes are characteristic of Trojans, possibly reflecting a difference in composition and collisional evolution with respect to the main-belt asteroid population. *Binzel and Sauter* (1992) also reported the presence of high lightcurve amplitudes from a sample of 31 objects. In particular, they found that the amplitudes were significantly larger than in the main belt but only for objects larger than about 90 km. *Barucci et al.* (2002a) reported the results of a large survey obtained by a team of observers on an unbiased sample of 72 Trojans down to an absolute magnitude H ~ 10.2. Combined with existing data, these increase the number of known periods and amplitudes to 75 Trojans, most of which are in the diameter range 70–150 km. The mean rotation frequency of this sample (f = 2.14 ± 0.12 rev/day) is statistically indistinguishable from the main belt (f = 2.26 ± 0.14 rev/day), but the Trojan distribution is well fit by a Maxwellian, unlike the main belt.

The few known spin axes of Trojans seem to be randomly distributed, and include both prograde- and retrograde-sense rotations (*Barucci et al.,* 2002a). All these results suggest that the Trojan population has undergone a higher degree of collisional evolution than the main belt.

The lightcurve amplitude also gives some indication of the elongation of the body. Assuming a triaxial ellipsoid shape with semiaxes a > b > c and no albedo variation, the estimation of the lower limit of the semiaxis ratio can be derived

$$a/b = 10^{0.4\Delta m}$$

The amplitude, however, varies considerably depending on the unknown aspect angle under which the observations are made, with the amplitude being largest for an equatorial aspect, and smallest with a polar aspect. The simple inversion tends to underestimate the maximum amplitudes, and therefore the a/b ratio, for objects that are observed only once. This ambiguity can be removed by obtaining lightcurves at multiple epochs. Nevertheless, even reducing the amplitudes to the aspect of 60° in the case of multiple observations to eliminate bias effects, the Trojans appear (at the 99% confidence level) to have a larger mean amplitude than the main-belt objects. This implies more elongated shapes for the Trojan population.

3.2. Albedo and Diameters

Albedo and diameters of Jupiter Trojans are still relatively poorly known. The widest data sample in this field was published by *Fernández et al.* (2003). On the basis of midinfrared and visible observations, they radiometrically derived V-band geometric albedo and radii of 32 Jupiter Trojans. No statistically significant correlation between albedo and radius has been found. The midinfrared colors seem to support a thermal behavior of "slow rotators" with a thermal inertia no greater than about half that of the Moon and similar to the limits found for some of the Centaurs. Figure 2 shows the albedo distribution of Jupiter Trojans, together with those of active comets and dead comet candidates. The mean value, as well as the standard deviation, depends on the value of an empirical term, η, called the beaming parameter, which enters into the equations for the temperature of the asteroid's surface. The beaming parameter acts as a proxy of both surface roughness and thermal inertia (a measure of the resistance of the surface to changes in temperature), and can vary over factors of several (see additional discussion in chapter by Stansberry et al.). Lack of knowledge of the albedo and η leads to uncertainty in the surface temperature, and dominates the uncertainties in size as estimated from a thermal flux measurement. In the case of Jupiter Trojans, with η = 0.94, the computed mean albedo value is 0.041 ± 0.002 (with a standard deviation of 0.007), while with the standard value of 0.756 the mean albedo increases to 0.056 ± 0.003. The albedo distribution, found by *Fernández et al.* (2003), is narrower than the one derived from IRAS measurements. With a beaming parameter close to 1 it becomes consistent with that of comets, but it does not match the albedo values of Centaurs and TNOs published since 2003 (reported in the chapter by Stansberry et al.). According to *Fernández et al.* (2003) this could imply that the Jupiter Trojan surfaces are probably more like those of active and post-active comets, than like those of the pre-active ones (e.g., Centaurs). Only one object, 4079 Ennomos, has been found to have a high albedo, about 14σ away from the mean value. This could be due to the presence on the surface of this body of pristine ices, excavated from a subsurface layer by a recent collision. Alternatively, Ennomos could have a more "standard" albedo but a very unusual thermal inertia.

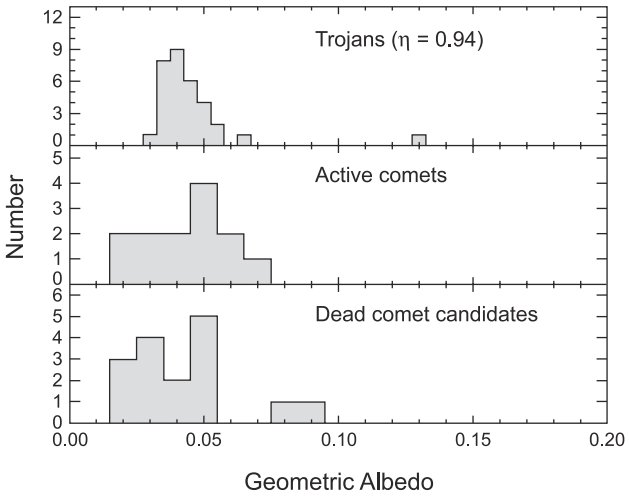

Fig. 2. Comparison of Trojan albedos with those of active comets and dead comet candidates (by *Fernández et al.,* 2003).

3.3. Density

Whereas the aspects treated in the previous sections concern only the surface properties, the densities can give information on the similarities (or differences) between the objects' bulk physical properties. However, one should keep in mind the caveat that bodies with related origin can have different densities. For instance, in the Kuiper belt, the density of Pluto is larger than that of Varuna, because the former probably underwent some sort of differentiation and lost some volatile material.

We know the bulk density of two Trojan objects: 617 Patroclus and 624 Hektor. Patroclus is the first discovered binary Trojan (*Merline et al.,* 2001). A preliminary orbital determination allowed a first estimate of a bulk density of ~1.3 g/cm^3 (*Merline et al.,* 2002; *Noll,* 2006), similar to that of C-type asteroids (see *Britt et al.,* 2002, for a review). *Marchis et al.* (2006a) have taken several observations of Patroclus using the laser guide star adaptive optics at Keck. These observations provided better measurements of the period and the orbital distance of the two components, which in turn allows the determination of the masses. Using the thermal measurements of *Fernández et al.* (2003) to estimate the sizes of the components, *Marchis et al.* (2006a) concluded that the bulk density of this object is ~0.8 g/cm^3. This is a very low density, compared to any other asteroid known so far. However, it is close to the bulk densities of 1–2 g/cm^3 inferred for Kuiper belt objects (*Jewitt and Sheppard,* 2002; *Lacerda and Luu,* 2006).

Recent observations of 624 Hektor with adaptive optics techniques have revealed a moonlet orbiting a primary that appears to be a close-in or contact binary (*Marchis et al.,* 2006b). Masses determined from the orbit of the moonlet and from modeling the stability of the binary primary agree, and both result in a density of ~2.4 g/cm^3 for Hektor.

The densities of Trojans appear to span a broad range that includes estimated densities of main-belt asteroids [0.6–3.8 g/cm^3 (*Noll,* 2006)], comet nuclei [0.1–1.5 g/cm^3 (chapter by Lowry et al.)], and TNOs [0.6–2.5 g/cm^3 (chapter by McKinnon et al.)]. This range of densities may indicate that the Trojans are a mixture of objects from different source populations, or could reflect the collisional environment in the Trojan swarms (i.e., some low-density rubble piles and some coherent impact fragments or undisrupted primitive bodies).

3.4. V + NIR Photometry and Spectroscopy

The physical properties and the surface composition of Jupiter Trojans are not at present well known. Visible photometry is available from SDSS data for about 300 objects (*Szabó et al.,* 2007). Visible spectra are available for less than 150 objects (*Jewitt and Luu,* 1990; *Vilas et al.,* 1993; *Fitzsimmons et al.,* 1994; *Lazzarin et al.,* 1995; *Bendjoya et al.,* 2004; *Fornasier et al.,* 2004; *Lazzaro et al.,* 2004; *Fornasier et al.,* 2007), while near-infrared spectra have been published for about 50 bodies (*Jones et al.,* 1990; *Luu et al.,* 1994; *Dumas et al.,* 1998; *Cruikshank et al.,* 2001; *Emery and Brown,* 2003; *Dotto et al.,* 2006; *Yang and Jewitt,* 2006). All the observed Trojans appear spectrally featureless: The large majority of them can be classified in the asteroid taxonomy (*Tholen and Barucci,* 1989) as belonging to the D class, but P and C types are also present among them. In particular, no indication of hydration bands, as seen in some asteroids (*Vilas and Gaffey,* 1989; *Vilas et al.,* 1994) and in several small bodies of the solar system (see review by *de Bergh et al.,* 2004), is in the Trojan spectra. The visible spectral slopes range from –1% to 25%/10^3 Å, while for TNOs the visible slopes span between –1% and 55%/10^3 Å (chapter by Barucci et al.).

Although Jupiter Trojans are believed to be formed in a region rich in frozen volatiles, water ice is still undetected in their spectra. *Emery and Brown* (2003, 2004) published 0.3–4.0-μm spectra of 17 bodies and also presented models of the surface composition (see Fig. 3). They did not detect water ice and hydrated silicate features in their V + NIR spectra and they estimated upper limits of a few percent and up to 30% respectively for these materials at the surface. More recently, *Yang and Jewitt* (2006) published near-infrared spectra and models of the surface composition of five Jupiter Trojans, assessing at less than 10% the total amount of water ice present on their surface.

Several mechanisms can be invoked to explain this lack of water ice on the surface of the observed objects (assuming they contained water ice to begin with). Laboratory experiments have shown that space-weathering processes on the icy surfaces of atmosphereless bodies can produce an irradiation mantle spectrally red and with low albedo (*Moore et al.,* 1983; *Thompson et al.,* 1987; *Strazzulla,* 1998; *Hudson and Moore,* 1999). In the scenario suggested by *Morbidelli et al.* (2005), Jupiter Trojans could have been devolatized during their high-eccentricity phase, when cometary activity should have been intense. Alternatively, they could have formed a dust mantle as suggested by *Tancredi et al.* (2006) for kilometer-sized comet nuclei. Therefore, water ice, originally present on the surface of Jupiter Trojans, would be now completely covered and ice signatures would be now detectable only if inner fresh material would be exposed by recent collisions.

Unfortunately, the observations of Jupiter Trojans belonging to dynamical families have shown no spectral features related to the presence of ices on the surface of the observed bodies. *Dotto et al.* (2006) published visible and near-infrared (0.5–2.5 μm) spectra of 24 Jupiter Trojans belonging to dynamical families, also presenting models of the surface composition (as an example, Fig. 4 shows the spectra obtained for the Makhaon family). The most important characteristic they found is the uniformity of the Trojan population. All the investigated dynamical families appear quite similar in surface composition, without any peculiar difference. No relation exists between spectral properties and dimensions of the bodies, and some small differences in the spectral behaviors can be explained by different degrees of space-weathering alteration. All the investigated

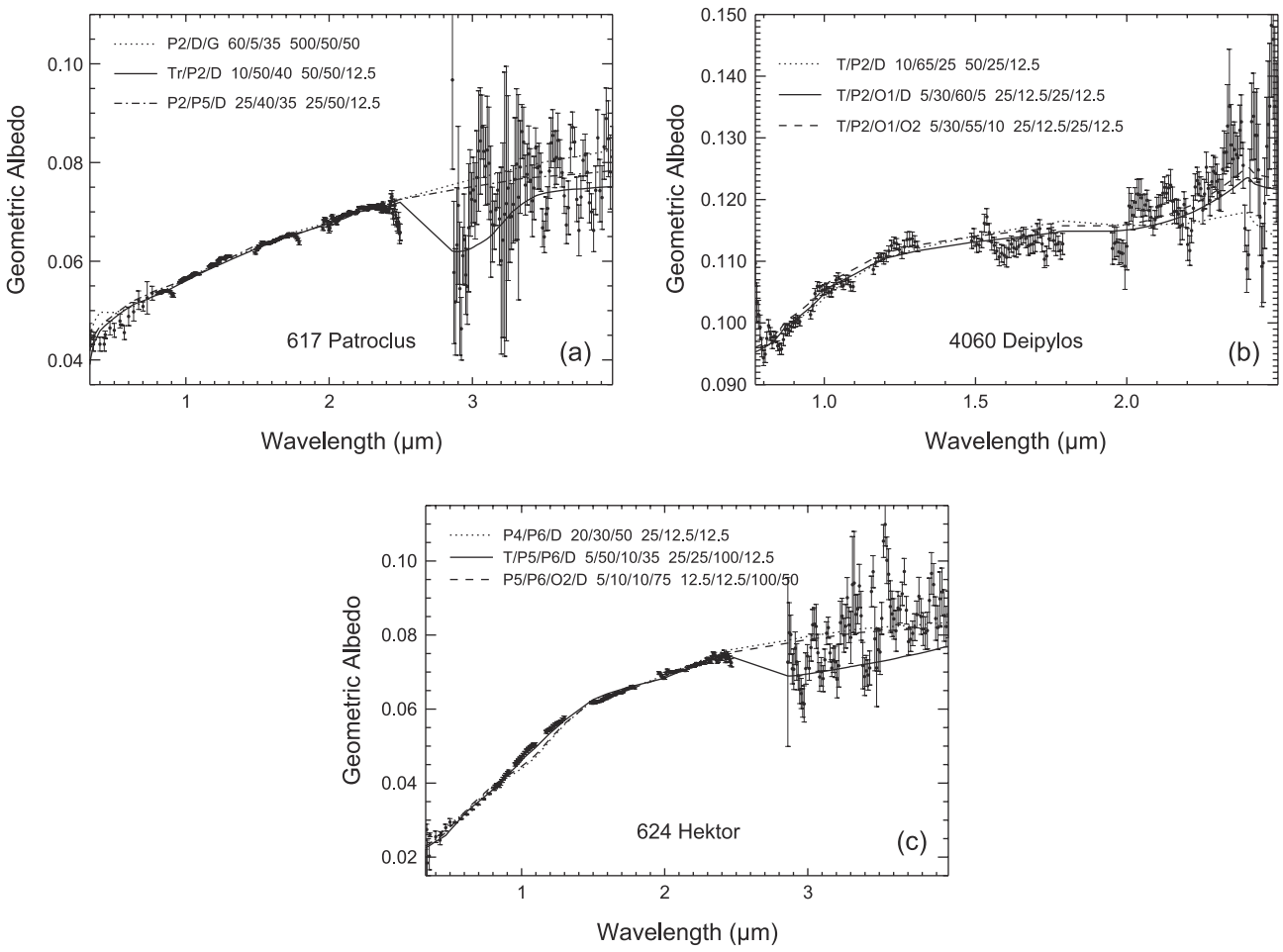

Fig. 3. V + NIR spectra and models of the surface composition of three Jupiter Trojans. The one- or two-digit codes represent the following materials: P2 to P8 — glassy silicates with pyroxene stoichiometry, O1 and O2 — glassy silicate with olivine stoichiometry, D — amorphous carbon, G — graphite, T — Titan tholin. The first set of numbers following the codes are mixing ratios, and the second set are grain diameters in micrometers (see *Emery and Brown,* 2004, for more details).

Trojans have featureless spectra. No diagnostic features that would enable distinguishing the family members from the background objects of the Trojan population have been detected. Importantly, no signatures of water ice have been observed in the spectra of these bodies.

Fornasier et al. (2007), analyzing the spectral slopes of Jupiter Trojans as a function of the orbital elements, found a color-inclination trend with bluer objects at lower i. In their sample this trend is completely dominated by the L_4 Eurybates family, a compact core inside the Menelaus family (*Beaugé and Roig,* 2001) (see also the P.E.Tr.A. Project at *www.daf.on.br/ froig/petra/*). Eurybates constitutes a peculiar case among the families analyzed so far, since the spectral behavior of its members is quite homogeneous: The spectral slopes are strongly clustered around S = 2%/10^3 Å, with the highest S values corresponding to the smaller objects (D < 25 km). The visible spectra of the Eurybates family members (see Fig. 5) are very similar to those of C-type main-belt asteroids, of the less-red Centaurs, and of cometary nuclei. This family could be produced by the fragmentation of a very peculiar parent body, whose origin must be still assessed or, alternatively, could be an old family, where space-weathering processes have flattened all the spectra, covering any original differences in composition among the different members. In this last case we would have the first observational evidence of objects whose spectra have been flattened by space-weathering processes and, according to the scenario suggested by *Moroz et al.* (2004), the composition of the parent body of such a family would have been rich in complex hydrocarbons. Unfortunately, we do not know the age of this dynamical family and we do not have infrared spectra of Eurybates members. Further observations in an enlarged wavelength range and numerical simulations are absolutely needed to investigate and definitively assess the nature and the origin of this very peculiar family. Dynamical families belonging to the L_4 swarm seem to have a more heterogeneous composition than those of the L_5 swarm, since a higher presence of C and P types is

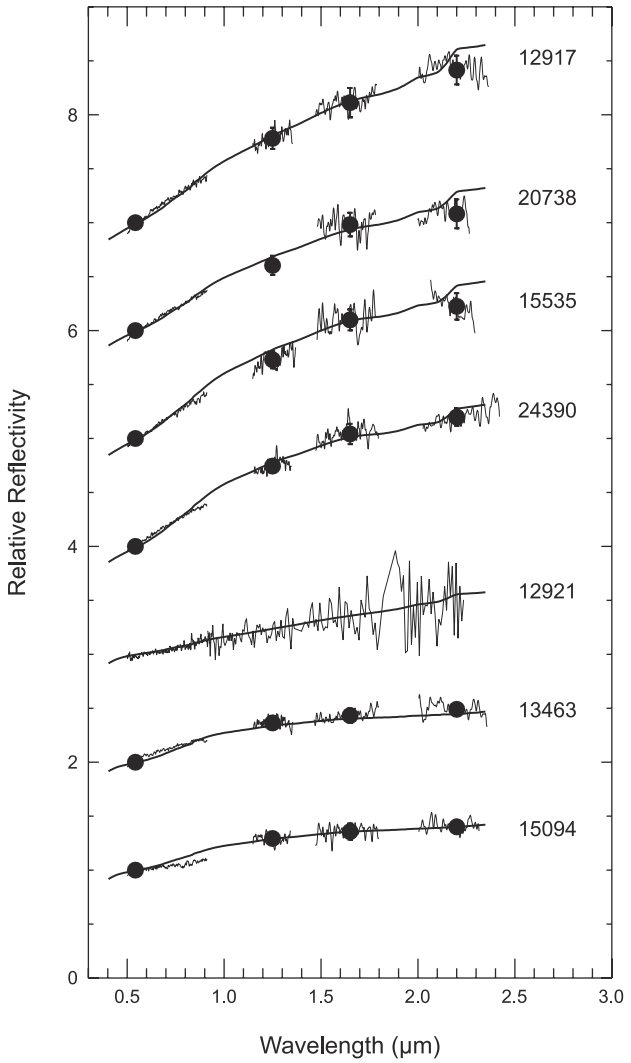

Fig. 4. V + NIR spectra and models of the surface composition of the members of the Makhaon family (by *Dotto et al.,* 2006). All the spectra are normalized at 0.55 μm and shifted for clarity.

observed among the L_4 objects (*Fornasier et al.,* 2007). Moreover, the dynamical families belonging to the L_4 cloud are more robust than those of the L_5, surviving as densely populated clustering at low relative velocity cutoff. This could suggest that the L_4 cloud is more collisionally evolved than the L_5, but it is still too early to give an interpretation of this in terms of the composition of the two cloud populations, since we cannot exclude that still unobserved C- and P-type families are present also in the L_5 cloud.

Szabó et al. (2007), on the basis of the SDSS observations, found also that the color of Trojans is correlated with the orbital inclination (with redder objects and larger inclination) and did not detect any difference between the L_4 and L_5 swarms.

Fornasier et al. (2007) also performed a comparison of the whole sample of Jupiter Trojans' spectral slopes and (B, V, R, I, J, H, and K) colors available in the literature, with those of small bodies of the outer solar system: comets, scattered TNOs, classical disk objects, and Plutinos. They found that the Trojan mean colors are compatible with those of the short-period comets. Nevertheless, the widths of their color distributions are incompatible, as well as the shapes of the distributions. The compatibility in color is possibly caused by the small size of the short-period comet sample rather than by a physical similarity. Trojans do not have any of the ultrared slopes seen on many Centaurs and TNOs. Their average colors are fairly similar to those of the neutral/less-red Centaurs, but the overall distributions are not compatible.

3.5. Thermal Emission Observations

The majority of measurements of thermal emission from Trojan asteroids are broadband photometric observations for the purpose of determining sizes and albedos, as described in section 3.2. Spectroscopic observations of Trojans in the thermal-IR have not been possible from the ground due to strong telluric absorptions, bright and rapidly varying sky background, and the inherent faintness of Trojans due to their distance from the Sun. The sensitivity of the ISO satellite was also insufficient for thermal-IR spectroscopy of Trojans. The Infrared Spectrograph (IRS) on the Spitzer Space Telescope is more sensitive, however, and *Emery et al.* (2006a) have recently reported 5.2–37-μm thermal emission spectroscopy of three Trojan asteroids: 624 Hektor, 911 Agamemnon, and 1172 Aneas.

The flux density at each wavelength measured by IRS (also called the spectral energy distribution, or SED) de-

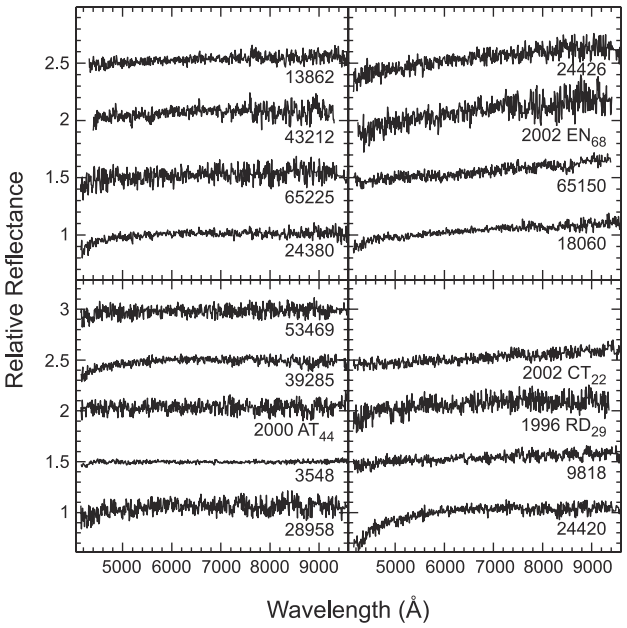

Fig. 5. Visible spectra of the members of the Eurybates family (by *Fornasier et al.,* 2007). All the spectra are normalized at 0.55 μm and shifted for clarity.

pends on the Trojan's size, composition, and surface temperature distribution. This last term is in turn dependent on several factors, including distance from the Sun, albedo, surface roughness, and thermal inertia. Spectral features in the SED are superposed on the thermal continuum, which must be removed with the use of a physical model. *Emery et al.* (2006a) employed a modified version of the standard thermal model (STM) as well as a more advanced thermophysical model, which includes the effects of thermal inertia. Fits of these models to the data result in estimates of physical parameters such as size, albedo, and thermal inertia (see chapter by Stansberry et al.). The sizes and albedos derived from the IRS spectra are in agreement with previous estimates. The Trojan data are consistent with zero thermal inertia, although the thermophysical models allow thermal inertias of these Trojan asteroids of up to about 5 J m^{-2} $s^{-1/2}$ K^{-1} for reasonable values of surface roughness (in these units, thermal inertia is ~50 for the Moon, ~15 for large main-belt asteroids, and ~2500 for bare rock).

Emissivity spectra are derived by dividing the measured SED by the modeled thermal continuum. The emissivity spectra of Hektor, Agamemnon, and Aneas are shown in Fig. 6. Compositional features evident in these spectra include an emission plateau at about 9.1–11.5 μm and a broader emission high from about 18–28 μm. More subtle features include possible peaks near 19 μm and near 24 μm and another emissivity rise near 34 μm. The Trojan spectra broadly resemble the emissivity spectra of some carbonaceous meteorites and fine-grained silicates (Fig. 7).

Coarse-grained silicates exhibit emissivity lows instead of highs near 10 and 20 μm, and therefore cannot explain the data. Upon closer comparison with fine-grained materials, however, several differences are also apparent: The 10-μm plateau is narrower for the Trojans, their spectra do not rise as sharply near 15 μm. Emissivity spectra of two low-albedo main-belt asteroids (10 Hygiea and 308 Polyxo) from ISO exhibit similarly narrow 10-μm emission plateaus (*Barucci et al.,* 2002b; *Dotto et al.,* 2004). No minerals in available spectral libraries resolve these differences, nor do linear mixtures of up to five components.

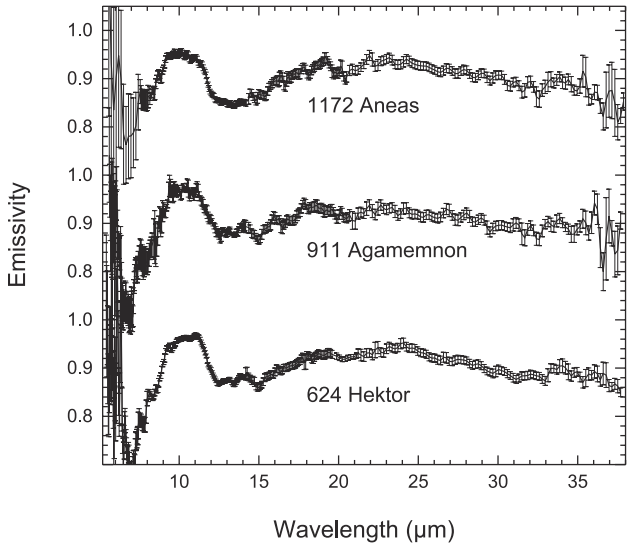

Fig. 6. Emissivity spectra of Aneas, Agamemnon, and Hektor from *Emery et al.* (2006a). The shortest wavelength portion (λ < 7.5 μm) of the Aneas spectrum has been binned by a factor of 5 to improve the S/N.

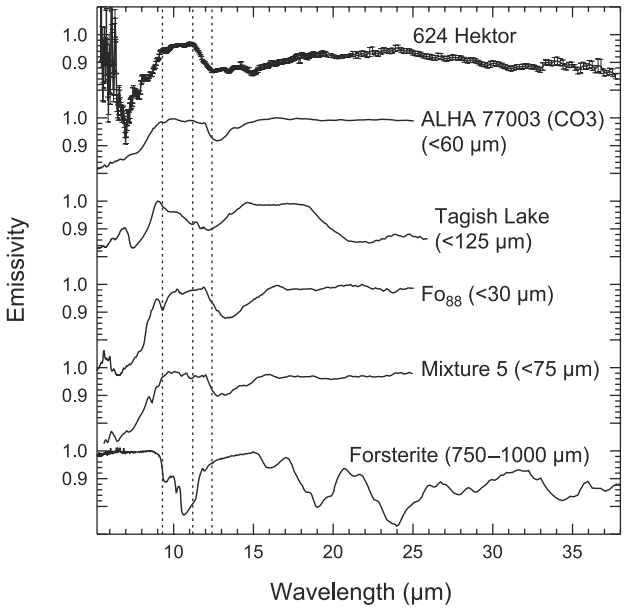

Fig. 7. Emissivity spectra of meteorites, minerals, and mixtures. Grain sizes are listed in parentheses. Mixture 5 is 63% Fo_{92} + 28% enstatite + 4% muscovite + 2% pyrophyllite + 3% calcite.

Emery et al. (2006a) suggest three hypotheses for the differences between the Trojan asteroid data and expected regolith emissivity spectra. The first is that the Trojans support comet-like comae. This hypothesis is rejected because no comae are apparent in deep optical and thermal-IR images of these objects. The second possibility is that a fine-grained, low-density regolith with a fairy castle structure emits in a manner similar to an extended coma, perhaps from extreme porosity. The third hypothesis is that fine-grained silicates are imbedded in a matrix of material that is relatively transparent in the midinfrared. Both of these latter two hypotheses imply a significant fraction of fine-grained silicates on the surfaces, and the last requires an additional matrix material. The presence and spectral dominance of silicates on the surfaces of Trojan asteroids is consistent with some modeling of V + NIR reflectance spectra of Trojans (*Cruikshank et al.,* 2001; *Emery and Brown,* 2004) that rely on silicates rather than organics to provide the red spectral slope, but *Emery et al.* (2006b) show that extension of the V + NIR models to the thermal-IR does not match the measured Trojan emissivity spectra. Additional analysis exploring the effects of surface structure (porosity and particles embedded in a transparent matrix) while simultaneously conforming to the constraints imposed by

both V + NIR reflectance spectra and the thermal-IR emissivity spectra will likely provide further insight into the composition of Trojan surfaces.

4. DISCUSSION AND CONCLUSION

On the basis of the presently available data, it seems that Jupiter Trojans constitute a very homogeneous population whose members have featureless and neutral to moderately red V + NIR spectra. No differences have been found among members of dynamical families and background objects and no relations have been found among spectral properties and dimensions. A very peculiar case is given by the Eurybates family, which shows a peculiar abundance of spectrally flat objects, similar to C-type main-belt asteroids or to the neutral/less-red Centaurs. A correlation seems to exist between colors and inclinations, with redder objects at higher inclinations. The presence of more robust dynamical families in the L_4 cloud seems to suggest that it is more collisionally evolved than the L_5.

According to the most recent models on the origin and early evolution of Jupiter Trojans, Centaurs, and TNOs, some similarities among the different populations of minor bodies of the outer solar system would be expected. Nevertheless, the rotational properties, albedo distributions, and spectral characteristics of Jupiter Trojans are only partially in agreement with the analogous characteristics of the other populations. Jupiter Trojans are characterized by larger-amplitude lightcurves, implying elongated shapes and a higher degree of collisional evolution compared to the population of larger TNOs (see chapter by Sheppard et al.), but this is probably just a size effect. Albedo, color, and visible spectral slope distributions of Jupiter Trojans are very different from those of TNOs, comets, and Centaurs: Jupiter Trojans are among the less-red objects within these populations and have the narrowest color distribution. While their mean colors are compatible with those of the short-period comets, the width of their color distributions is not, nor is the shape. Likewise, the Trojan average colors are similar to those of the neutral/less-red Centaurs, but the overall color distributions are not statistically compatible. Unfortunately, V + NIR reflectance spectra of Trojan asteroids do not exhibit absorption features that would provide direct clues to their surface composition. These featureless spectra rule out significant amounts of water ice, hydrated silicates, crystalline anhydrous silicates such as those apparent on main-belt asteroids, certain organic materials (those with strong K- and L-band absorptions, typically from many aliphatic bonds), and other simple ices (e.g., CH_3OH, H_2O, CH_4, SO_2). But for determination of specific composition, we are left to ask what materials produce featureless spectra with neutral to moderately red spectral slopes. *Gradie and Veverka* (1980) suggested macromolecular organic materials, and subsequent spectral modeling has proven that such materials do an excellent job of matching Trojan asteroid spectra shortward of 2.5 μm (e.g., *Dotto et al.,* 2006). However, *Emery and Brown* (2004) reported that they could not simultaneously match the red spectral slope at $\lambda < 2.5$ μm and the absence of absorptions in the L band (2.8–4.0 μm) with these organics (tholins), and conclude that organics cannot be responsible for the red spectral slopes unless some organic exists that has a red slope, but no L-band absorptions. They used amorphous silicates to model the red slopes of Trojans, but *Emery et al.* (2006b) noted that these models do not successfully reproduce midinfrared emissivity spectra of Trojans.

Fine-grained silicates have recently been detected in thermal emission spectra of three Trojan asteroids (*Emery et al.,* 2006a). These represent the first discrete mineralogical signatures detected for Trojans. Models of emissivity spectra of regoliths are not yet sophisticated enough to determine specific silicate mineralogy, but the Trojan emissivity spectra between 5.2 and 37 μm are qualitatively similar to those of comets (e.g., *Crovisier et al.,* 1997; *Stansberry et al.,* 2004; *Lisse et al.,* 2006) and some Centaurs (chapter by Barucci et al.), but distinct from many main-belt asteroids (*Emery et al.,* 2005). The grain size for the Trojan silicates (less than a few micrometers) is smaller than can be modeled with the techniques generally used to model reflectance spectra (*Hapke,* 1981, 1993; *Shkuratov et al.,* 1999) (both based on geometric optics). This indicates that new techniques are necessary for proper modeling of reflectance data.

As already noted by *Fernández et al.* (2003), it seems that Jupiter Trojans are more similar to the active and post-active comets than to the non-active icy bodies (Centaurs and TNOs). This is compatible with the scenario suggested by *Morbidelli et al.* (2005), where Jupiter Trojans, before being captured in the region where they currently reside, temporarily had large eccentricities that brought them relatively close to the Sun, where cometary activity should have been intense. The major problem with this scenario is due to the information we have on Jupiter Trojans belonging to dynamical families. These objects were separated from the parent body when it was already in one of the Lagrangian clouds, where they are still observable. As a consequence, if a family is not very old, we must be able to see on the surface of the fragments the internal composition of the progenitor. In this context is hard to explain why we do not see any ice signature on the spectra of family members, if the progenitor originally contained ices in the interior, as expected. Objects formed at large heliocentric distances must contain ices on their interior and it is still unknown what mechanism could completely hide the ice content on the surface of the small fragments.

Knowledge of the ages of the Trojan dynamical families would be helpful on this topic and it is of fundamental importance in the interpretation of the data on the C-type spectrally neutral objects belonging to the Eurybates family. We still cannot assess if (1) this is a very old family, where space-weathering processes flattened the spectra covering the primordial ices; (2) it is a young family produced by an object spectrally similar to C-type asteroids or neutral/less-red Centaurs; or (3) it is a young family where irradiation mantles formed in a timescale shorter than the family age.

The comparison among the spectral properties of Jupiter Trojans, TNOs, cometary nuclei, and Centaurs is difficult to interpret. These objects do not all look the same. These differences could mean that there are no relationships among these populations or that their surfaces have been modified in different ways. From dynamical modeling we are quite confident that there is a link among three of these populations: TNOs are the source, Centaurs are the transient population, and comets are the end members in the transfer chain. Unfortunately, the observational constraints are at present too weak to determine the origin of Jupiter Trojans, and these objects remain among the most intriguing bodies of the solar system.

As anticipated in section 2, the two models on the origin of Jupiter Trojans, local capture vs. capture from a distant disk, allow us to interpret similarities and differences between Trojans and TNOs in very different ways. If the Trojans have been captured from the local planetesimal population, then they represent relatively unaltered samples of the middle part of the solar nebula. We have no other direct samples from this region that not only fed a growing Jupiter, but also probably contained the "snow-line" marking the onset of H_2O condensation and may have supported formation of nebular organics via Fischer-Tropsch-type catalytic reactions. In this scenario, we might expect Trojan compositions consistent with the *Gradie and Tedesco* (1982) paradigm of the trend of asteroid composition with heliocentric distance (i.e., low-temperature silicates, organics, some water ice). It is somewhat unclear what primordial TNO compositions are implied by this scenario, but perhaps some TNOs could also have originated in this region and/or at slightly larger distances and would therefore have similar compositions to Trojans, while more distant objects were more compositionally distinct. Or, conversely, the various types of space weathering could have affected the evolution of surfaces in this region differently than other regions. These scenarios are qualitatively consistent with observational results that Trojans are similar to some taxonomic classes of Centaurs and TNOs as well as some classes of outer main-belt asteroids. It also predicts compositional differences between Trojans and TNOs formed at larger distances. Conversely, if one accepts the *Morbidelli et al.* (2005) scenario, both Trojans and TNOs come from the primordial transneptunian disk. They are therefore genetically related, although they might have formed in slightly different parts of the aforementioned disk. Therefore, the physical similarities between Trojans and TNOs appear normal, whereas the differences need to be explained on the basis of the subsequent physical evolutions of bodies stored at different places.

Of course, a detailed comparison between the physical properties of Trojans and TNOs can also help to distinguish between the two formation models, although it is probably too early to reach a conclusion at this stage. Further observations are absolutely needed to constrain the composition of Jupiter Trojans and to look for Eurybates-like families in other regions of the orbital parameter phase space. A larger sample of V + NIR spectra would be useful to investigate the nature of more objects, especially looking for spectral features related to the presence of water ice on their surfaces. Polarimetric observations could help to investigate the surface structure (grain size and porosity). Numerical simulations would be useful to assess the age of the known families, in order to investigate the effects of space-weathering processes on the surface of these atmosphereless bodies formed at large heliocentric distances and, as a consequence, to constrain their primordial composition.

REFERENCES

Barucci M. A., Cruikshank D. P., Mottola S., and Lazzarin M. (2002a) Physical properties of Trojan and Centaur asteroids. In *Asteroids III* (W. F. Bottke Jr. et al., eds.), pp. 273–287. Univ. of Arizona, Tucson.

Barucci M. A. and 12 colleagues (2002b) 10 Hygiea: ISO infrared observations. *Icarus, 156,* 202–210.

Beaugé C. and Roig F. (2001) A semianalytical model for the motion of the Trojan asteroids: Proper elements and families. *Icarus, 153,* 391–415.

Bendjoya P., Cellino A., Di Martino M., and Saba L. (2004) Spectroscopic observations of Jupiter Trojans. *Icarus, 168,* 374–384.

Binzel R. P. and Sauter L. M. (1992) Trojan, Hilda, and Cybele asteroids: New lightcurve observations and analysis. *Icarus, 95,* 222–238.

Britt D. T., Yeomans D., Housen K., and Consolmagno G. (2002) Asteroid density, porosity, and structure. In *Asteroids III* (W. F. Bottke Jr. et al., eds.), pp. 485–500. Univ. of Arizona, Tucson.

Crovisier J., Leech K., Bockelée-Morvan D., Brook T. Y., Hanner M. S., Altieri B., Keller H. U., and Lellouch E. (1997) The spectrum of Comet Hale-Bopp (C/1995 O1) observed with the Infrared Space Observatory at 2.9 astronomical units from the sun. *Science, 275,* 1904–1907.

Cruikshank D. P., Dalle Ore C. M., Roush T. L., Geballe T. R., Owen T. C., de Bergh C., Cash M. D., and Hartmann W. K. (2001) Constraints on the composition of Trojan asteroid 624 Hektor. *Icarus, 153,* 348–360.

de Bergh C., Boehnhardt H., Barucci M. A., Lazzarin M., Fornasier S., Romon-Martin J., Tozzi G. P., Doressoundiram A., and Dotto E. (2004) Aqueous altered silicates at the surface of two Plutinos? *Astron. Astrophys., 416,* 791–798.

Dotto E., Barucci M. A., Brucato J. R., Mueller T. G., and Carvano J. (2004) Polyxo: ISO-SWS spectrum up to 26 micron. *Astron. Astrophys., 427,* 1081–1084.

Dotto E., Fornasier S., Barucci M. A., Licandro J., Boehnhardt H., Hainaut O., Marzari F., de Bergh C., and De Luise F. (2006) The surface composition of Jupiter Trojans: Visible and near-infrared survey of dynamical families. *Icarus, 183,* 420–434.

Dumas C., Owen T., and Barucci M. A. (1998) Near-infrared spectroscopy of low-albedo surfaces of the solar system: Search for the spectral signature of dark material. *Icarus, 133,* 221–232.

Dunlap J. L. and Gehrels T. (1969) Minor planets. III. Lightcurves of a Trojan asteroid. *Astron. J., 74,* 797–803.

Emery J. P. and Brown R. H. (2003) Constraints on the surface composition of Trojan asteroids from near-infrared (0.8–4.0 μm) spectroscopy. *Icarus, 164,* 104–121.

Emery J. P. and Brown R. H. (2004) The surface composition of Trojan asteroids: Constraints set by scattering theory. *Icarus, 170,* 131–152.

Emery J. P., Cruikshank D. P., and Van Cleve J. (2005) Thermal emission spectroscopy of asteroids with the Spitzer Space Telescope. *Bull. Am. Astron. Soc., 37,* 15.07.

Emery J. P., Cruikshank D. P., and Van Cleve J. (2006a) Thermal emission spectroscopy (5.2–38 μm) of three Trojan asteroids with the Spitzer Space Telescope: Detection of fine-grained silicates. *Icarus, 182,* 496–512.

Emery J. P., Cruikshank D. P., and Van Cleve J. (2006b) Structure and composition of the surfaces of Trojan asteroids from reflection and emission spectroscopy (abstract). In *Lunar and Planetary Science XXXVII,* Abstract #2075. Lunar and Planetary Institute, Houston (CD-ROM).

Fernández J. A. and Ip W.-H. (1984) Some dynamical aspects of the accretion of Uranus and Neptune — The exchange of orbital angular momentum with planetesimals. *Icarus, 58,* 109–120.

Fernández Y. R., Sheppard S. S., and Jewitt D. J. (2003) The albedo distribution of jovian Trojan asteroids. *Astron. J., 126,* 1563–1574.

Fitzsimmons A., Dahlgren M., Lagerkvist C.-I., Magnusson P., and Williams I. P. (1994) A spectroscopic survey of D-type asteroids. *Astron. Astrophys., 282,* 634–642.

Fleming H. J. and Hamilton D. P. (2000) On the origin of the Trojan asteroids: Effects of Jupiter's mass accretion and radial migration. *Icarus, 148,* 479–493.

Fornasier S., Dotto E., Marzari F., Barucci M. A., Boehnhardt H., Hainaut O., and de Bergh C. (2004) Visible spectroscopic and photometric survey of L_5 Trojans: Investigation of dynamical families. *Icarus, 172,* 221–232.

Fornasier S., Dotto E., Hainaut O., Marzari F., Boehnhardt H., De Luise F., and Barucci M. A. (2007) Visible spectroscopic and photometric survey of Jupiter Trojans: Final results on dynamical families. *Icarus, 190,* 622–642.

Giorgilli A. and Skokos C. (1997) On the stability of Trojan asteroids. *Astron. Astrophys., 317,* 254–261.

Gomes R. S. (1997) Dynamical Effects of planetary migration on the primordial asteroid belt. *Astron. J., 114,* 396–401.

Gomes R. S., Morbidelli A., and Levison H. F. (2004) Planetary migration in a planetesimal disk: Why did Neptune stop at 30 AU? *Icarus, 170,* 492–507.

Gomes R., Levison H. F., Tsiganis K., and Morbidelli A. (2005) Origin of the cataclysmic late heavy bombardment period of the terrestrial planets. *Nature, 435,* 466–469.

Gradie J. C. and Tedesco E. F. (1982) Compositional structure of the asteroid belt. *Science, 216,* 1405–1407.

Gradie J. C. and Veverka J. (1980) The composition of the Trojan asteroids. *Nature, 283,* 840–842.

Hahn J. M. and Malhotra R. (1999) Orbital evolution of planets embedded in a planetesimal disk. *Astron. J., 117,* 3041–3053.

Hahn J. M. and Malhotra R. (2005) Neptune's migration into a stirred-up Kuiper belt: A detailed comparison of simulations to observations. *Astron. J., 130,* 2392–2414.

Hapke B. (1981) Bidirectional reflectance spectroscopy. I — Theory. *J. Geophys. Res., 86,* 3039–3054.

Hapke B. (1993) *Theory of Reflectance and Emittance Spectroscopy.* Cambridge Univ., New York. 455 pp.

Hartmann W. K., Tholen D. J., Goguen J., Binzel R. P., and Cruikshank D. P. (1988) Trojan and Hilda asteroid lightcurves. I. Anomalously elongated shapes among Trojans (and Hildas?). *Icarus, 73,* 487–498.

Hartmann W. K., Ryder G., Dones L., and Grinspoon D. (2000) The time-dependent intense bombardment of the primordial Earth/Moon system. In *Origin of the Earth and Moon* (R. M. Canup and K. Righter, eds.), pp. 493–512. Univ. of Arizona, Tucson.

Hudson R. L. and Moore M. H. (1999) Laboratory studies of the formation of methanol and other organic molecules by water + carbon monoxide radiolysis: Relevance to comets, icy satellites, and interstellar ices. *Icarus, 140,* 451–461.

Ivezić Ž. and 32 colleagues (2001) Solar system objects observed in the Sloan Digital Sky Survey commissioning data. *Astron. J., 122,* 2749–2784.

Jewitt D. C. and Luu J. X. (1990) CCD spectra of asteroids. II — The Trojans as spectral analogs of cometary nuclei. *Astron. J., 100,* 933–944.

Jewitt D. C. and Sheppard S. S. (2002) Physical properties of trans-neptunian object (20000) Varuna. *Astron. J., 123,* 2110–2120.

Jewitt D. C., Trujillo C. A., and Luu J. X. (2000) Population and size distribution of small jovian Trojan asteroids. *Astron. J., 120,* 1140–1147.

Jones T. D., Lebofsky L. A., Lewis J. S., and Marley M. S. (1990) The composition and origin of the C, P, and D asteroids — Water as a tracer of thermal evolution in the outer belt. *Icarus, 88,* 172–192.

Lacerda P. and Jewitt D. (2006) Densities from lightcurves. *Bull. Am. Astron. Soc., 38,* 34.02.

Lacerda P. and Luu L. (2006) Analysis of the rotational properties of Kuiper belt objects. *Astron. J., 131,* 2314–2326.

Lazzarin M., Barbieri C., and Barucci M. A. (1995) Visible spectroscopy of dark, primitive asteroids. *Astron. J., 110,* 3058–3072.

Lazzaro D., Angeli C. A., Carvano J. M., Mothé-Diniz T., Duffard R., and Florczak M. (2004) S3OS2: The visible spectroscopic survey of 820 asteroids. *Icarus, 172,* 179–220.

Levison H. F. and Duncan M. J. (1997) From the Kuiper belt to Jupiter-family comets: The spatial distribution of ecliptic comets. *Icarus, 127,* 13–32.

Levison H., Shoemaker E. M., and Shoemaker C. S. (1997) The dispersal of the Trojan asteroid swarm. *Nature, 385,* 42–44.

Lisse C. M. and 16 colleagues (2006) Spitzer spectral observations of the Deep Impact ejecta. *Science, 313,* 635–640.

Luu J. X., Jewitt D., and Cloutis E. (1994) Near-infrared spectroscopy of primitive solar system objects. *Icarus, 109,* 133–144.

Malhotra R. (1993) The origin of Pluto's peculiar orbit. *Nature, 365,* 819–821.

Malhotra R. (1995) The origin of Pluto's Orbit: Implications for the solar system beyond Neptune. *Astron. J., 110,* 420–429.

Marchis F. and 17 colleagues (2006a) A low density of 0.8 g cm^{-3} for the Trojan binary asteroid 617 Patroclus. *Nature, 439,* 565–567.

Marchis F., Wong M. H., Berthier J., Descamps P., Hestroffer D., Vachier F., Le Mignant D., and De Pater I. (2006b) S/2006 (624) 1. *IAU Circular 8732*.

Marzari F. and Scholl H. (1998a) The growth of Jupiter and Saturn and the capture of Trojans. *Astron. Astrophys., 339,* 278–285.

Marzari F. and Scholl H. (1998b) Capture of Trojans by a growing proto-Jupiter. *Icarus, 131,* 41–51.

Marzari F. and Scholl H. (2000) The role of secular resonances in the history of Trojans. *Icarus, 146,* 232–239.

Merline W. J., Close L. M., Menard F., Dumas C., Chapman C. R., and Slater D. C. (2001) Search for asteroid satellites. *Bull. Am. Astron. Soc., 33,* 1133.

Merline W. J., Weidenschilling S. J., Durda D. D., Margot J. L., Pravec P., and Storrs A. D. (2002) Asteroids do have satellites.

In *Asteroids III* (W. F. Bottke Jr. et al., eds.), pp. 289–312. Univ. of Arizona, Tucson.

Milani A. (1993) The Trojan asteroid belt: Proper elements, stability, chaos and families. *Cel. Mech. Dyn. Astron., 57,* 59–94.

Milani A. and Knežević Ž. (1994) Asteroid proper elements and the dynamical structure of the asteroid main belt. *Icarus, 107,* 219–254.

Michtchenko T. A., Beaugé C., and Roig F. (2001) Planetary migration and the effects of mean motion resonances on Jupiter's Trojan asteroids. *Astron. J., 122,* 3485–3491.

Moore M. H., Donn B., Khanna R., and A'Hearn M. F. (1983) Studies of proton-irradiated cometary-type ice mixtures. *Icarus, 54,* 388–405.

Morbidelli A., Levison H. F., Tsiganis K., and Gomes R. (2005) Chaotic capture of Jupiter's Trojan asteroids in the early solar system. *Nature, 435,* 462–465.

Moroz L., Baratta G., Strazzulla G., Starukhina L., Dotto E., Barucci M. A., Arnold G., and Distefano E. (2004) Optical alteration of complex organics induced by ion irradiation: 1. Laboratory experiments suggest unusual space weathering trend. *Icarus, 170,* 214–228.

Noll K. S. (2006) Solar system binaries. In *Asteroids Comets Meteors 2005* (D. Lazzaro et al., eds.), pp. 301–318. IAU Symposium 229, Cambridge Univ., Cambridge.

Peale S. J. (1993) The effect of the nebula on the Trojan precursors. *Icarus, 106,* 308–322.

Petit J.-M., Morbidelli A., and Chambers J. (2001) The primordial excitation and clearing of the asteroid belt. *Icarus, 153,* 338–347.

Pollack J. B., Hubickyj O., Bodenheimer P., Lissauer J. J., Podolak M., and Greenzweig Y. (1996) Formation of the giant planets by concurrent accretion of solids and gas. *Icarus, 124,* 62–85.

Rabe E. (1965) Limiting eccentricities for stable Trojan librations. *Astron. J., 70,* 687–688.

Rivkin A. S., Binzel R. P., Howell E. S., Bus S. J., and Grier J. A. (2003) Spectroscopy and photometry of Mars Trojans. *Icarus, 165,* 349–354.

Robutel P. and Gabern F. (2006) The resonant structure of Jupiter's Trojan asteroids — I. Long-term stability and diffusion. *Mon. Not. R. Astron. Soc., 372,* 1463–1482.

Scholl H., Marzari F., and Tricarico P. (2005) Dynamics of Mars Trojans. *Icarus, 175,* 397–408.

Sheppard S. S. and Trujillo C. (2006a) A survey for Trojan asteroids of Saturn, Uranus and Neptune. *Bull. Am. Astron. Soc., 38,* 44.03.

Sheppard S. S. and Trujillo C. (2006b) A thick cloud of Neptune Trojans and their colors. *Science, 313,* 511–514

Shoemaker E. M., Shoemaker C. S., and Wolfe R. F. (1989) Trojan asteroids: Populations, dynamical structure and origin of the L_4 and L_5 swarms. In *Asteroids II* (R. P. Binzel et al., eds.), pp. 487–523. Univ. of Arizona, Tucson.

Shkuratov Y., Starukhina L., Hoffmann H., and Arnold G. (1999) A model of spectral albedo of particulate surfaces: Implications for optical properties of the Moon. *Icarus, 137,* 235–246.

Stansberry J. A. and 17 colleagues (2004) Spitzer observations of the dust coma and nucleus of 29P/Schwassmann-Wachmann 1. *Astrophys. J. Suppl. Ser., 154,* 463–468.

Strazzulla G. (1998) Chemistry of ice induced by bombardment with energetic charged particles. In *Solar System Ices* (B. Schmitt et al., eds.), pp. 281–301. Kluwer, Dordrecht.

Szabó Gy. M., Ivezić Ž., Jurić M., and Lupton R. (2007) The properties of jovian Trojan asteroids listed in SDSS Moving Object Catalog 3. *Mon. Not. R. Astron. Soc., 377,* 1393–1406.

Tancredi G., Fernández J. A., Rickman H., and Licandro J. (2006) Nuclear magnitudes and size distribution of Jupiter family comets. *Icarus, 182,* 527–549.

Tholen D. J. and Barucci M. A. (1989) Asteroid taxonomy. In *Asteroids II* (R. P. Binzel et al., eds.), pp. 298–315. Univ. of Arizona, Tucson.

Thompson W. R., Murray B. G. J. P. T., Khare B. N., and Sagan C. (1987) Coloration and darkening of methane clathrate and other ices by charged particle irradiation — Applications to the outer solar system. *J. Geophys. Res., 92,* 14933–14947.

Tsiganis K., Gomes R., Morbidelli A., and Levison H. F. (2005) Origin of the orbital architecture of the giant planets of the solar system. *Nature, 435,* 459–461.

Vilas F. and Gaffey M. J. (1989) Phyllosilicate absorption features in main-belt and outer-belt asteroid reflectance spectra. *Science, 246,* 790–792.

Vilas F., Larson S. M., Hatch E. C., and Jarvis K. S. (1993) CCD reflectance spectra of selected asteroids. II. Low-albedo asteroid spectra and data extraction techniques. *Icarus, 105,* 67–78.

Vilas F., Jarvis K. S., and Gaffey M. J. (1994) Iron alteration minerals in the visible and near-infrared spectra of low-albedo asteroids. *Icarus, 109,* 274–283.

Wetherill G. W. (1992) An alternative model for the formation of the asteroids. *Icarus, 100,* 307–325.

Yang B. and Jewitt D. (2006) Spectroscopic search for water ice on jovian Trojan asteroids. *Bull. Am. Astron. Soc., 38,* 50.03.

Yoshida F. and Nakamura T. (2005) Size distribution of faint jovian L_4 Trojan asteroids. *Astron. J., 130,* 2900–2911.

Yoshida F., Nakamura T., Watanabe J., Kinoshita D., Yamamoto N., and Fuse T. (2003) Size and spatial distributions of sub-km main-belt asteroids. *Publ. Astron. Soc. Japan, 55,* 701–715.